Letter

Spin splitting and disorder of Landau levels in HgTe-based Dirac fermions

D. A. Kozlov [1,2] J. Ziegler,[1] N. N. Mikhailov [2] Z. D. Kvon,[2,3] and D. Weiss [1]

[1]*Experimental and Applied Physics, University of Regensburg, D-93040 Regensburg, Germany*
[2]*Rzhanov Institute of Semiconductor Physics, 630090 Novosibirsk, Russia*
[3]*Department of Physics, Novosibirsk State University, 630090 Novosibirsk, Russia*

This study conducts experimental exploration into a system of two-dimensional Dirac fermions utilizing a critical-thickness HgTe quantum well in weak magnetic fields. The formation and evolution of Shubnikov–de Haas oscillations in the magnetotransport and the capacitive response are studied, complemented by calculations of Landau levels (LLs). It is shown that the behavior of the LLs is influenced not only by the linear dispersion law of the carriers and the Zeeman splitting, but also by the splitting of the Dirac cones in zero magnetic field caused by interface inversion asymmetry. The measured value of the splitting is 1.5 meV. The behavior of the zero LL is studied and its spin splitting is demonstrated. It is shown that the broadening of the zero LL is several times higher than that of the other levels due to the lack of charge impurity screening.

Massless Dirac fermion systems, similar to graphene, can be realized in HgTe quantum wells with a critical thickness of $6.3 \ldots 6.6$ nm. At this thickness the energy spectrum changes from direct to inverted [1]. Such systems are of interest because of their linear dispersion law and their strong spin-orbit interaction. In this system classical transport [2–6], quantum transport [1,3,7–12], and cyclotron resonance [13–17] were investigated, the density of states (DoS) was measured [18], and the quantization of the Faraday rotation was discovered [19].

Although numerous methods have been applied and diverse results have been obtained, with a considerable body of work dedicated to band structure and Landau level (LL) calculations [1,14,15,20–25], the experimental data currently available on the characteristics of these levels remains remarkably incomplete. On the one hand, the study of cyclotron resonance has allowed us to confirm the existence of the Dirac spectrum and the nonequidistance of LLs [13,14,16]. On the other hand, the cyclotron resonance obeys selection rules prohibiting spin flips when the orbital number changes by 1. It is, therefore, insensitive to Zeeman splitting. Magnetotransport measurements are not subject to these limitations. However, previous research has primarily focused on the quantum Hall effect (QHE) in high magnetic fields [8,10] or on the hole side, where Fermi-level pinning and the observation of ultralong QHE plateaus for Dirac holes are observed due to the presence of side valleys with heavy holes [9,12]. At the same time, the region of weak magnetic fields, where the features of the Dirac spectrum should be most evident, is virtually unexplored experimentally.

The charge neutrality point is of particular interest. In quantizing magnetic fields, the zero LL is a characteristic fingerprint of the Dirac fermion system [26,27]. In graphene, due to the presence of two valleys and spin, it is fourfold degenerate, but because of the interaction effects the degeneracy can be lifted [28]. However, due to the small magnitude of the interaction effects and the small value of the g factor, the

degeneracy lifting is observed at rather high magnetic fields. In the QHE regime, the conductivity of graphene at the Dirac point can be due to both the weakly conducting bulk and the counterpropagating dissipative edge states [29]. A different behavior can be expected in HgTe Dirac fermion quantum wells because of the large Zeeman splitting, which could open a gap at the Dirac point. The QHE near the charge neutrality point has been studied in detail in semimetallic HgTe quantum wells (QWs) [30,31] and, to a lesser extent, in QWs of critical thickness [6,11] or close to it [32], but with a focus on strong magnetic fields or mesoscopic samples. Thus, the behavior of the system of Dirac fermions at the charge neutrality point at the transition from weak to quantizing magnetic fields remains poorly understood.

The present work focuses on the study of Landau levels in a (013)-oriented 6.6-nm-thick HgTe quantum well [see Fig. 1(a)] in quantizing but relatively weak (less than 3 Tesla) magnetic fields at temperatures of 1.5–10 K. We performed combined magnetotransport and capacitance measurements. Due to the high sensitivity of the transport measurements and the possibility to measure the DoS directly by the capacitive technique, we were able to study the zero LL in detail and to demonstrate its splitting in a strong field. The samples investigated were ten-pin gated Hall bars with a size of 450×50 µm and a total capacitance of 36 pF. Magnetotransport measurements were performed using a four-terminal scheme with lock-in detection at a frequency of 4–12 Hz and a drive current of 10–100 nA, which prevents heating effects. The capacitive measurements were performed according to a scheme similar to that described in [18,33]: a small oscillating voltage V_{ac} was applied to the gate at frequency f against a constant bias V_g, while the quantum well was at zero potential. The magnitude of the AC current, phase-shifted by 90 degrees with respect to the AC voltage, reflected the capacitance of the structure. The parameters V_{ac}, f, and T were varied as a function of the magnetic field in order to eliminate both resistive effects and the effect of DoS smearing by temperature and drive voltage,
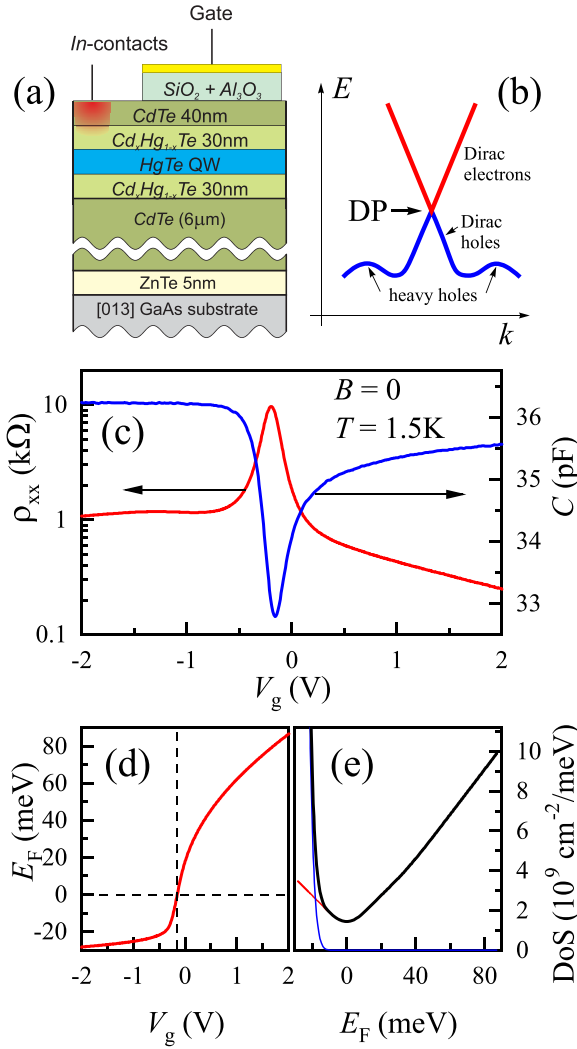
FIG. 1. (a) Cross section of the investigated structure. (b) Schematic band structure of the system. While the conduction band consists of simple spin-degenerate Dirac cones, the valence band has both a region with a linear dispersion law (Dirac holes) and side valleys with heavy holes. The side valleys in the valence band are located ≈25 meV below the Dirac point. (c) Gate voltage dependence of the longitudinal resistance ρ_{xx} (red line, left axis) and the capacitance (blue line, right axis) at $B = 0$ and $T = 1.5$ K. (d), (e) Fermi energy vs gate voltage (d) and the DoS vs Fermi energy (e) extracted from the capacitance data.

while achieving the highest possible signal-to-noise ratio. The parameters used were $V_{ac} = 20 \ldots 100$ mV, $f = 83 \ldots 4$ Hz, $T = 1.5 \ldots 10$ K, where the first number of the respective range corresponds to zero magnetic field and the second one to $B = 3$ T.

The measured dependencies of $\rho_{xx}(V_g)$ and $C(V_g)$ are shown in Fig. 1(c). The Dirac point (DP) is located at $V_g = -0.18$ V near the maximum of ρ_{xx} and the minimum of C. As one moves away from the DP to the right, the electron density in the system increases and a smooth decrease in resistance and increase in capacitance is observed. From the measured capacitance and following the previously developed approach [18], we extracted the dependencies of the Fermi energy E_F
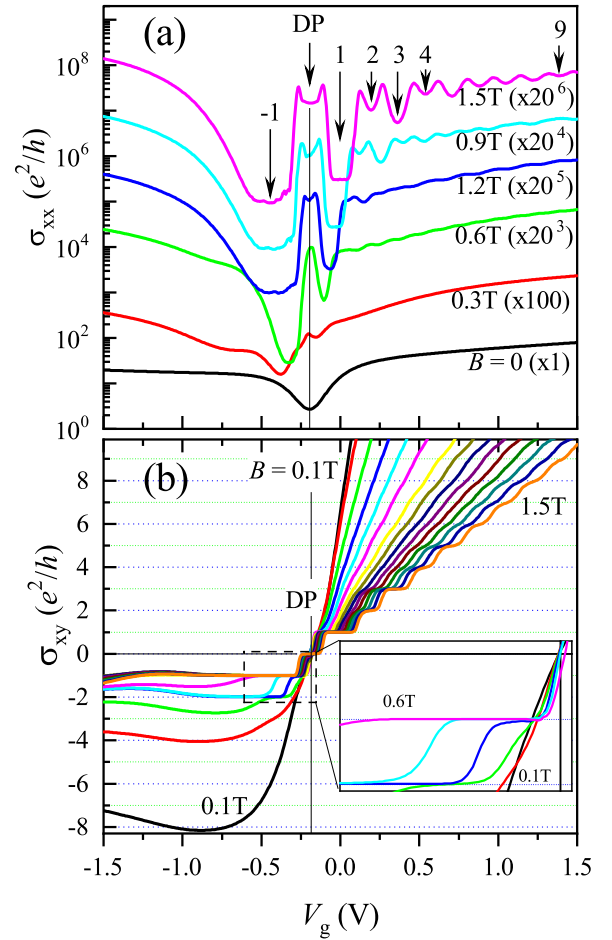
FIG. 2. (a) Gate voltage dependence of the longitudinal conductivity σ_{xx}, measured for $B = 0$, $0.3 \ldots 1.5$ T, and $T = 1.5$ K. For clarity, curves measured at nonzero magnetic fields are multiplied by the factor shown in parentheses. The minima and corresponding filling factors are indicated by the numbered vertical arrows. (b) Gate voltage dependence of the Hall conductivity σ_{xy}, measured for $B = 0.1 \ldots 1.5$ T in steps of 0.1 T. In both panels, "DP" denotes the Dirac point. The inset: the zoomed region shows the formation of the first hole plateau. The experimental data are shown only in the range of $0.1 \ldots 0.6$ T.

[Fig. 1(d)] and the DoS [Fig. 1(e)] on the gate voltage. On the electron side, we can clearly see that the DoS depends almost linearly on the Fermi energy. It reaches a value of 80 meV at $V_g = 2$ V. On the left side of the DP, Dirac holes coexist with heavy holes [9,12,18]. The presence of heavy holes leads to a rapid increase of the DoS, and thus to the pinning of the Fermi level at about -25 meV below the DP [Fig. 1(d)], and causes the measured capacitance to saturate to the value of the geometric capacitance [Fig. 1(c)].

Figure 2 shows the dependencies of the conductivity tensor components $\sigma_{xx}(V_g)$ and $\sigma_{xy}(V_g)$ in magnetic fields up to 1.5 T, calculated by tensor inversion from the measured ρ_{xx} and ρ_{xy} data. These dependencies show a transition from classical transport to the QHE regime, accompanied by the formation of a series of distinct minima in σ_{xx} and plateaus in σ_{xy}. The most striking effect is the strong asymmetry between electrons and holes: first, the QHE on the hole side is formed

in a magnetic field of only 0.4 T (and even at 0.15 T when measured at lower temperatures [9]), while on the electron side it requires twice the field. Second, the plateaus on the hole side are anomalously long, and from 0.7 to 1.5 T, only one plateau with fixed $\sigma_{xy} = -e^2/h$ is observed. Both features are explained by the coexistence of Dirac (light) and heavy holes: while the former are responsible for the formation of the plateaus, the latter are localized and play a role of charge reservoir [9,12,34]. The anomalous length of the plateau is related to the exchange of light and heavy holes, implementing the QHE reservoir model. A similar effect was later discovered in graphene on some substrates and is known as "giant QHE" [35]. The second feature, i.e., the formation of the plateau at ultralow fields, is associated with the effect of an increased quantum lifetime of Dirac holes in comparison to the Dirac electrons in the presence of the heavy holes. The heavy holes, due their high value of the effective mass and the valley degeneracy, are characterized by a very high DoS value. In turn, the efficiency of charge impurities screening is proportional to the DoS, resulting in a reduced scattering rate of the Dirac holes and a significant increase of their quantum lifetime.

The QHE on the electron side in Fig. 2(b) shows up to five electronic plateaus of σ_{xy}, which become blurred for higher filling factors. This behavior reflects the peculiarity of Dirac fermion systems, where the distance between neighboring LLs decreases with increasing ν. It could be explained by the magnetic field dependence of the LLs in the simplest approximation, fitted to the four-zone Bernevig-Hughes-Zhang (BHZ) Hamiltonian [1,22],

$$E_n^{\pm}(B) = \alpha\sqrt{nB} \pm g\mu_B B/2, \tag{1}$$

where $n = 0, 1, 2 \ldots$ is the Landau quantum number, $\alpha = 25$ meV $T^{-1/2}$ is a numerical coefficient, $g = 50$ is the effective g factor, μ_B is the Bohr magneton, with $g\mu_B = 3.5$ meV T^{-1}, and $\pm$ denotes different spin orientations. From formula (1) it can be seen that in weak magnetic fields the distance between Landau gaps characterized by odd filling factors is larger than the distance between spin-split gaps (even filling factor), with the maximum distance for filling factor $\nu = 1$. These calculations agree with the experimental $\sigma_{xx}(V_g)$ values at $B = 1.5$ T [Fig. 2(a)]: the deepest minima of the conductances are observed at $\nu = 1$ and $\nu = 3$, while the minima at $\nu = 2, 4$, and 6 are significantly less deep. At higher filling factors, the amplitude of the conductivity oscillations associated with even and odd filling factors become equal. For the most accurate calculation it is necessary to use the more complicated six- or even eight-band Kane Hamiltonian [20,23]. However, on the electron side and in weak magnetic fields (below 2 T), very similar results are obtained with all three approaches.

Let us analyze the behavior of the measured conductivity oscillations in the limit of weak magnetic fields. Figure 3(b) shows a two-dimensional map of the second derivative of the conductance with respect to the gate voltage $d^2\sigma_{xx}(B, V_g)/dV_g^2$. From the depth of the minima at different filling factors, one can estimate the size of the corresponding energy gap. The red and magenta dots in Fig. 3 indicate the points B_ν where minima of the conductivity with filling factor ν first occur. For odd filling factors (red dots), a clear trend of
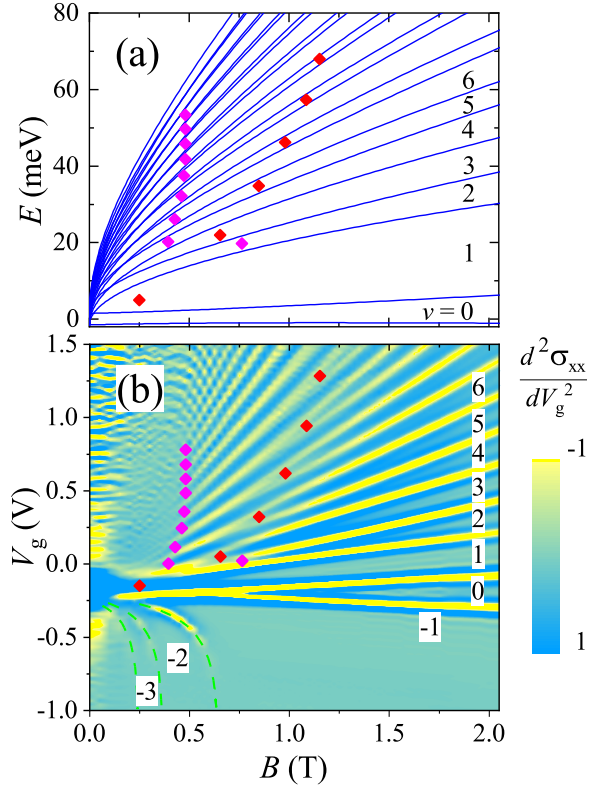
FIG. 3. (a) LLs calculated on the basis of the BHZ model with interface inversion asymmetry taken into account with cone splitting $\gamma = 1.5$ meV [24,25]. Numbers denote filling factors, counting the number of occupied Landau levels. The magnetic field axis is the same as in panel (b). (b) Two-dimensional map of the second derivative $d^2\sigma_{xx}(B, V_g)/dV_g^2$. The blue color corresponds to minima of σ_{xx}, yellow to maxima. Numbers, as in panel (a), denote the corresponding filling factors. Green dashed lines mark the behavior of Dirac holes LLs [12]. In both panels the dots indicate the points B_ν where the minima of the conductivity oscillations with the filling factor ν appear first: red dots correspond to odd filling factors, magenta dots correspond to even ones. The position B_1 of the first red dot was determined from the $\sigma_{xx}(V_g)$ data in Fig. 2.

B_ν toward increasing B with increasing ν is observed. This is consistent with formula (1) and reflects the decreasing energy gap for larger ν. The behavior of B_ν for even filling factors (magenta dots), reflecting spin gaps, turns out to be less trivial. For $\nu = 2$ the gap opens at a field of 0.8 T, which exceeds both $B_1 = 0.25$ T and $B_3 = 0.65$ T and thus qualitatively agrees with the theoretical expectation described by Eq. (1). However, all subsequent spin gaps open in a magnetic field smaller than 0.5 T, i.e., 2–2.5 times smaller than the field for the neighboring odd filling factors.

In order to explain the observed behavior of the spin gaps, we performed the LL calculations based on the four-zone BHZ Hamiltonian with an additional factor taken into account, namely, the IIA asymmetry [24,25]. The asymmetry reflects the real atomistic structure of the quantum well and leads to the $B = 0$ Dirac cone splitting. The original BHZ Hamiltonian parameters (the band constants $\mathcal{A} = 373$ meV nm, $\mathcal{B} = -857$ meV nm^2, $\mathcal{D} = -682$ meV nm^2; the electron and hole g factors $g_E = 18.5$ and $g_H = 2.4$) were

taken from the paper of Büttner *et al.* [1]. The Dirac cone splitting amplitude γ was used as a single fitting parameter. The best fit was obtained for $\gamma = 1.5$ meV, and the result of the calculation is shown in Fig. 3(a). Note that the optimal value of γ varies from 1.3 to 1.7 meV for different energy ranges, giving an average value of 1.5 meV. When IIA is taken into account, the calculation agrees well with the experimental data. This is illustrated by the red and magenta dots in Fig. 3(a), which are taken from panel (b). It can be seen that the distance between neighboring LLs for odd (red) and even (magenta) filling factors are quite similar, if compared at same Fermi energy (i.e., the gap for $\nu = 5$ should be compared with $\nu = 8$). The comparison at the same energy is essential, because the efficiency of impurities screening and thus the LLs' broadening depend on energy. The magnitude of disorder has its maximum near the DP and can reach 10–15 meV [18].

To check the last assumption we studied the zero LL. The nature of the QHE state with $\nu = 0$ differs from all other QHE states with integer filling factors. In Dirac fermion systems, the $\nu = 0$ state may be formed either by a spin-degenerate half-occupied zero LL, or its degeneracy could be lifted because of the spin splitting [29]. However, in both cases the values of σ_{xx} and σ_{xy} tend to be zero due to bulk localization. Alternatively, the spin splitting of the zero LL could be accompanied by the formation of two counterpropagating (electron and hole) edge channels, which could enhance the conductivity. However, these channels are not protected from backscattering and therefore the conductivity remains low. Note that the double-peak structure of σ_{xx} shown in Fig. 2(a) stems from resistivity tensor inversion and is not a signature of spin splitting. Thus the local transport response turns out to be weakly sensitive to the Landau zero-level splitting. To solve this problem we used capacitive magnetospectroscopy, which directly probes the value of the DoS for arbitrary filling factors.

The results of the magnetocapacitance measurements $C(V_g)$ are shown in Fig. 4(a). The pronounced Shubnikov–de Haas (SdH) oscillations in $C(V_g)$ can only be observed from $B = 1.5$ T on due to the lower sensitivity compared to transport measurements. To improve the signal, the calculated differential signal $\delta C = C(V_g, B) - C(V_g, B = 0)$ is shown in Fig. 4(b). In the differential signal, the SdH oscillations start to appear at around 0.8 T. However, even at $B = 1$ T, not all gaps are resolved—only the largest Landau gaps with corresponding filling factors ν of 1 and 3 are observed, while the oscillations at higher gate voltages reflect the spin gaps with filling factors 6, 8, 10, and so on. The observed behavior is consistent with the magnetotransport data and the LL calculations. The absence of some minima can be explained by their smaller energy gaps.

The zeroth LL, a characteristic and the most remarkable footprint of Dirac fermions, appears in the capacitance signal already at $B = 0.2$ T and is the dominant maximum in Fig. 4(b). However, at fields below 1 T there is not even a hint of Zeeman splitting. The zeroth LL becomes clearly visible as a separate maximum in the nondifferential capacitance signal only from $B = 2$ T on. At this field all SdH oscillation minima except $\nu = 0$ and 2 are already resolved. Finally, the splitting of the zeroth LL appears at $B \sim 3$ T, where a small and broad
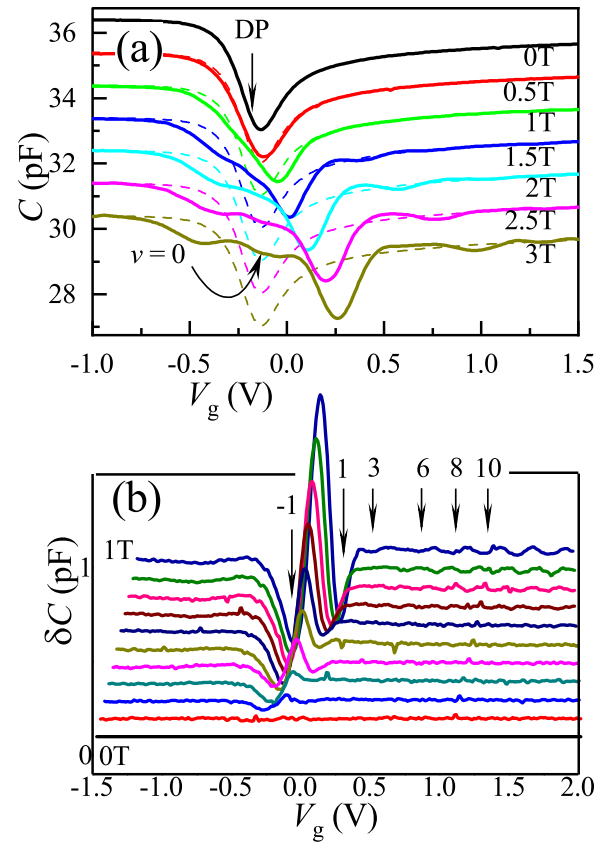
FIG. 4. (a) Gate voltage dependence of the capacitance C, measured at $B = 0, 0.5 \ldots 3$ T and $T = 1.5 - 10$ K. For clarity, the curves are shifted vertically. Dashed lines show the zero-field traces as a guide. The Dirac point "DP" is marked by a vertical arrow, "$\nu = 0$" marks the local capacitance minima, associated with the zeroth Landau-level splitting at $B = 3$ T. (b) The differential capacitance $\delta C(V_g, B) = C(V_g, B) - C(V_g, B = 0)$ measured at $B = 0, 0.1 \ldots 1$ T and $T = 1.5$ K. The curves for finite B are shifted both on the x and y axes to enhance visibility. The numbers denote the filling factors ν.

minimum can be observed close to the Dirac point. That the spin splitting of the zeroth LLs occurs at a significantly larger magnetic field than for any other one supports the hypothesis of stronger disorder and broadening. According to our calculations, the value of the spin gap for $\nu = 0$ at $B = 3$ T is around 10 meV, which is 2 times bigger then the gap for $\nu = 1$, clearly seen in the capacitance at $B = 1$ T. Note that the small deviation of the QW thickness from the critical value could open a small gap between valence and conduction bands also affecting the splitting of zero LL; however, our previous measurements at low temperatures up to 0.2 K [3,9] and zero magnetic field proved that this energy gap is absent or insignificant.

In summary, the experiments show that for odd filling factors ν the SdH oscillations are resolved at magnetic field values that increase monotonically with increasing ν. This is consistent with the simplest model [Eq. (1)] describing LLs in Dirac fermion systems. The behavior of SdH oscillations with even filling factors, i.e., those associated with spin gaps, differs significantly from the simplest model. First, SdH

oscillations with even filling factors of 6 and higher are formed in a magnetic field that is 2–2.5 times smaller than the field required to form neighboring SdH oscillations with odd filling factors. Second, the oscillations for small even ν appear at much stronger fields, reaching its maximum for $\nu = 0$ at a magnetic field of $\sim$3 T. The observed spin gaps are explained by the presence of an interface inversion asymmetry [24,25] with a magnitude of $\gamma = 1.5$ meV and enhanced disorder at the Dirac point. The obtained value of γ is almost an order

of magnitude smaller than expected from an interfacial atomistic calculation [24], but it qualitatively agrees with a recent THz spectroscopy study [15] with an even smaller value of 0.6 meV.

[1] B. Büttner, C. X. Liu, G. Tkachov, E. G. Novik, C. Brüne, H. Buhmann, E. M. Hankiewicz, P. Recher, B. Trauzettel, S. C. Zhang, and L. W. Molenkamp, Single valley Dirac fermions in zero-gap HgTe quantum wells, Nat. Phys. **7**, 418 (2011).

[2] G. Tkachov, C. Thienel, V. Pinneker, B. Büttner, C. Brüne, H. Buhmann, L. W. Molenkamp, and E. M. Hankiewicz, Backscattering of Dirac fermions in HgTe quantum wells with a finite gap, Phys. Rev. Lett. **106**, 076802 (2011).

[3] D. A. Kozlov, Z. D. Kvon, N. N. Mikhailov, and S. A. Dvoretsky, Weak localization of Dirac fermions in HgTe quantum wells, JETP Lett. **96**, 730 (2013).

[4] A. A. Dobretsova, Z. D. Kvon, L. S. Braginskii, M. V. Entin, and N. N. Mikhailov, Mobility of Dirac electrons in HgTe quantum wells, JETP Lett. **104**, 388 (2016).

[5] A. A. Dobretsova, Z. D. Kvon, L. S. Braginskii, M. V. Entin, and N. N. Mikhailov, Gapless Dirac electron mobility and quantum time in HgTe quantum wells, Semiconductors **52**, 1468 (2018).

[6] G. M. Gusev, Z. D. Kvon, D. A. Kozlov, E. B. Olshanetsky, M. V. Entin, and N. N. Mikhailov, Transport through the network of topological channels in HgTe based quantum well, 2D Mater. **9**, 015021 (2022).

[7] M. Pakmehr, C. Bruene, H. Buhmann, L. W. Molenkamp, A. V. Stier, and B. D. McCombe, Landau levels and spin splitting in the two-dimensional electron gas of a HgTe quantum well near the critical width for the topological phase transition, Phys. Rev. B **90**, 235414 (2014).

[8] D. A. Kozlov, Z. D. Kvon, N. N. Mikhailov, S. A. Dvoretskii, S. Weishäupl, Y. Krupko, and J.-C. Portal, Quantum Hall effect in HgTe quantum wells at nitrogen temperatures, Appl. Phys. Lett. **105**, 132102 (2014).

[9] D. A. Kozlov, Z. D. Kvon, N. N. Mikhailov, and S. A. Dvoretsky, Quantum Hall effect in a system of gapless Dirac fermions in HgTe quantum wells, JETP Lett. **100**, 724 (2015).

[10] T. Khouri, M. Bendias, P. Leubner, C. Brüne, H. Buhmann, L. W. Molenkamp, U. Zeitler, N. E. Hussey, and S. Wiedmann, High-temperature quantum Hall effect in finite gapped HgTe quantum wells, Phys. Rev. B **93**, 125308 (2016).

[11] G. M. Gusev, D. A. Kozlov, A. D. Levin, Z. D. Kvon, N. N. Mikhailov, and S. A. Dvoretsky, Robust helical edge transport at ν=0 quantum Hall state, Phys. Rev. B **96**, 045304 (2017).

[12] G. M. Gusev, A. D. Levin, D. A. Kozlov, Z. D. Kvon, and N. N. Mikhailov, Quantum transport of Dirac fermions in HgTe gapless quantum wells, Nanomaterials **12**, 2047 (2022).

[13] Z. D. Kvon, S. N. Danilov, D. A. Kozlov, C. Zoth, N. N. Mikhailov, S. A. Dvoretskii, and S. D. Ganichev, Cyclotron resonance of Dirac fermions in HgTe quantum wells, JETP Lett. **94**, 816 (2012).

[14] P. Olbrich, C. Zoth, P. Vierling, K.-M. Dantscher, G. V. Budkin, S. A. Tarasenko, V. V. Bel'kov, D. A. Kozlov, Z. D. Kvon, N. N. Mikhailov, S. A. Dvoretsky, and S. D. Ganichev, Giant photocurrents in a Dirac fermion system at cyclotron resonance, Phys. Rev. B **87**, 235439 (2013).

[15] V. Dziom, A. Shuvaev, J. Gospodarič, E. G. Novik, A. A. Dobretsova, N. N. Mikhailov, Z. D. Kvon, Z. Alpichshev, and A. Pimenov, Universal transparency and asymmetric spin splitting near the Dirac point in HgTe quantum wells, Phys. Rev. B **106**, 045302 (2022).

[16] C. Zoth, P. Olbrich, P. Vierling, K.-M. Dantscher, V. V. Bel'kov, M. A. Semina, M. M. Glazov, L. E. Golub, D. A. Kozlov, Z. D. Kvon, N. N. Mikhailov, S. A. Dvoretsky, and S. D. Ganichev, Quantum oscillations of photocurrents in HgTe quantum wells with Dirac and parabolic dispersions, Phys. Rev. B **90**, 205415 (2014).

[17] J. Ludwig, Y. B. Vasilyev, N. N. Mikhailov, J. M. Poumirol, Z. Jiang, O. Vafek, and D. Smirnov, Cyclotron resonance of single-valley Dirac fermions in nearly gapless HgTe quantum wells, Phys. Rev. B **89**, 241406(R) (2014).

[18] D. A. Kozlov, M. L. Savchenko, J. Ziegler, Z. D. Kvon, N. N. Mikhailov, S. A. Dvoretskii, and D. Weiss, Capacitance spectroscopy of a system of gapless Dirac fermions in a HgTe quantum well, JETP Lett. **104**, 859 (2016).

[19] A. Shuvaev, V. Dziom, Z. D. Kvon, N. N. Mikhailov, and A. Pimenov, Universal Faraday rotation in HgTe wells with critical thickness, Phys. Rev. Lett. **117**, 117401 (2016).

[20] O. E. Raichev, Effective Hamiltonian, energy spectrum, and phase transition induced by in-plane magnetic field in symmetric HgTe quantum wells, Phys. Rev. B **85**, 045310 (2012).

[21] B. Scharf, A. Matos-Abiague, and J. Fabian, Magnetic properties of HgTe quantum wells, Phys. Rev. B **86**, 075418 (2012).

[22] B. A. Bernevig and S. C. Zhang, Quantum spin Hall effect, Phys. Rev. Lett. **96**, 106802 (2006).

[23] E. G. Novik, A. Pfeuffer-Jeschke, T. Jungwirth, V. Latussek, C. R. Becker, G. Landwehr, H. Buhmann, and L. W. Molenkamp, Band structure of semimagnetic $Hg_{1-y}Mn_yTe$ quantum wells, Phys. Rev. B **72**, 035321 (2005).

[24] S. A. Tarasenko, M. V. Durnev, M. O. Nestoklon, E. L. Ivchenko, J.-W. Luo, and A. Zunger, Split Dirac cones in HgTe/CdTe quantum wells due to symmetry-enforced level anticrossing at interfaces, Phys. Rev. B **91**, 081302(R) (2015).

[25] M. V. Durnev and S. A. Tarasenko, Magnetic field effects on edge and bulk states in topological insulators based on HgTe/CdHgTe quantum wells with strong natural interface inversion asymmetry, Phys. Rev. B **93**, 075434 (2016).

[26] Y. Zhang, Y. W. Tan, H. L. Stormer, and P. Kim, Experimental observation of the quantum Hall effect and Berry's phase in graphene, Nature (London) **438**, 201 (2005).

[27] L. A. Ponomarenko, R. Yang, R. V. Gorbachev, P. Blake, A. S. Mayorov, K. S. Novoselov, M. I. Katsnelson, and A. K. Geim, Density of states and zero Landau level probed through capacitance of graphene, Phys. Rev. Lett. **105**, 136801 (2010).

[28] G. L. Yu, R. Jalil, B. Belle, A. S. Mayorov, P. Blake, F. Schedin, S. V. Morozov, L. A. Ponomarenko, F. Chiappini, S. Wiedmann, U. Zeitler, M. I. Katsnelson, A. K. Geim, K. S. Novoselov, and D. C. Elias, Interaction phenomena in graphene seen through quantum capacitance, Proc. Natl. Acad. Sci. USA **110**, 3282 (2013).

[29] D. A. Abanin, K. S. Novoselov, U. Zeitler, P. A. Lee, A. K. Geim, and L. S. Levitov, Dissipative quantum Hall effect in graphene near the Dirac point, Phys. Rev. Lett. **98**, 196806 (2007).

[30] G. M. Gusev, E. B. Olshanetsky, Z. D. Kvon, N. N. Mikhailov, S. A. Dvoretsky, and J. C. Portal, Quantum Hall effect near the charge neutrality point in a two-dimensional electron-hole system, Phys. Rev. Lett. **104**, 166401 (2010).

[31] O. E. Raichev, G. M. Gusev, E. B. Olshanetsky, Z. D. Kvon, N. N. Mikhailov, S. A. Dvoretsky, and J. C. Portal, Unconventional Hall effect near charge neutrality point in a two-dimensional electron-hole system, Phys. Rev. B **86**, 155320 (2012).

[32] E. Y. Ma, M. R. Calvo, J. Wang, B. Lian, M. Mühlbauer, C. Brüne, Y.-T. Cui, K. Lai, W. Kundhikanjana, Y. Yang, M. Baenninger, M. König, C. Ames, H. Buhmann, P. Leubner, L. W. Molenkamp, S.-C. Zhang, D. Goldhaber-Gordon, M. A. Kelly, and Z.-X. Shen, Unexpected edge conduction in mercury telluride quantum wells under broken time-reversal symmetry, Nat. Commun. **6**, 7252 (2015).

[33] D. A. Kozlov, D. Bauer, J. Ziegler, R. Fischer, M. L. Savchenko, Z. D. Kvon, N. N. Mikhailov, S. A. Dvoretsky, and D. Weiss, Probing quantum capacitance in a 3D topological insulator, Phys. Rev. Lett. **116**, 166802 (2016).

[34] M. V. Yakunin, S. S. Krishtopenko, W. Desrat, S. M. Podgornykh, M. R. Popov, V. N. Neverov, S. A. Dvoretsky, N. N. Mikhailov, F. Teppe, and B. Jouault, Unconventional reentrant quantum Hall effect in a HgTe/CdHgTe double quantum well, Phys. Rev. B **102**, 165305 (2020).

[35] Z. R. Kudrynskyi, M. A. Bhuiyan, O. Makarovsky, J. D. Greener, E. E. Vdovin, Z. D. Kovalyuk, Y. Cao, A. Mishchenko, K. S. Novoselov, P. H. Beton, L. Eaves, and A. Patanè, Giant quantum Hall plateau in graphene coupled to an InSe van der Waals crystal, Phys. Rev. Lett. **119**, 157701 (2017).